PCCP

Modeling of ion transport processes in disordered solids: Monte Carlo simulations of the low-temperature particle dynamics in the random barrier model

Bernhard Roling

Institut für Physikalische Chemie and Sonderforschungsbereich 458 (DFG), Westfälische Wilhelms-Universität Münster, Schlossplatz 4/7, 48149 Münster, Germany

Received 11th June 2001, Accepted 7th September 2001
First published as an Advance Article on the web 23rd October 2001

One of the simplest models describing the ion transport in disordered ionic conductors on a microscopic level is the random barrier model. Using Monte Carlo techniques, we simulate, for the first time, the *low-temperature* particle dynamics in random barrier model systems with long-range Coulomb interactions between the mobile particles. The ac conductivity spectra of these model systems are compared to those of ion conducting glasses, and it is shown that model spectra and experimental spectra exhibit a number of common features. On the basis of these results, the influence of the Coulomb interactions on the low-temperature particle dynamics in the random barrier model is discussed.

1. Introduction

In almost all structurally disordered ionic conductors, the mobile ions show a subdiffusive behaviour on short time and length scales. That means that when the time-dependent mean square displacement of the mobile ions, $\langle r^2(t)\rangle$, is smaller than typically a few Å^2, the mean square displacement increases sublinearly with time. On longer time and length scales, the subdiffusive behaviour passes over into a diffusive behaviour with $\langle r^2(t)\rangle \propto t$. This can be concluded from the frequency-dependent electrical conductivity spectra of the ionic conductors in connection with the experimental finding that the Haven ratio is of the order of unity.[1–6]

For a theoretical description of the ion dynamics in such systems, one often considers the hopping dynamics of non-interacting or interacting particles in disordered potential landscapes. In almost any hopping model of this type, the particle dynamics on short time and length scales are characterized by subdiffusive motions. This was proved by Kimball and Adams.[7] Therefore, the simple experimental observation that the short-time ion dynamics in disordered conductors is subdiffusive does not allow specific conclusions on the shape of the disordered potential landscape or on the role interionic interactions play in the ion dynamics. In order to obtain information on the shape of the potential landscape or on the importance of interionic interactions, detailed analyses of the frequency, temperature and composition dependence of the ac conductivity spectra of ionic conductors are necessary.

The composition dependence can be nicely studied in ion conducting glasses where the composition can be varied continuously. The present author has analysed the ac conductivity of various single ion conducting oxide glasses (containing only one type of mobile ion) and has found the following characteristic features.[6,8,9]

(A) For a given glass, the real part of the ac conductivity spectra, $\sigma'(\nu)$, obeys the following scaling relation:

$$\frac{\sigma'(\nu)}{\sigma_{dc}} = F\left(\frac{\nu}{\sigma_{dc}T}\right). \quad (1)$$

Here, σ_{dc} denotes the temperature-dependent dc conductivity of the mobile ions. The function F is independent of temperature. In particular, at low number densities of mobile ions ($N_V \leq 10^{20}$ cm^{-3}) where the Haven ratio is unity,[1,4,5,10,11] eqn. (1) transforms directly into the following scaling relation for the mean square displacement of the mobile ions:[6]

$$\langle r^2(t)\rangle = f(D_0 t). \quad (2)$$

Here, D_0 denotes the coefficient of self-diffusion of the mobile ions which is related to the dc conductivity *via* the Nernst–Einstein relation $\sigma_{dc}T = N_V q^2 D_0/k$, N_V and q being the number density and the charge of the mobile ions, respectively, while k denotes Boltzmann's constant. Again, the function f does not depend on temperature T. This implies that the mean square displacement where the subdiffusive behaviour of the mobile ions crosses over into diffusive behaviour is also independent of temperature.[6] In the following, this typical mean square displacement will be denoted as $\langle r_{cr}^2\rangle$.

(B) At low number densities of mobile ions, the square root of this typical mean square displacement, $\sqrt{\langle r_{cr}^2\rangle}$, decreases with $x^{-1/3}$. Here, x is the alkali oxide content of the glass. This was observed for different alkali conducting glassy systems.[6,12,13]

(C) The scaling functions F and f depend only weakly on the alkali oxide content of the glasses. Usually, the transition from the frequency-independent dc conductivity at low frequencies to the dispersive conductivity at higher frequencies becomes more abrupt as the alkali oxide content increases.[8,9]

One of the simplest models that has been used to describe the ion dynamics in disordered ionic conductors is the 'random barrier model'. In this model, the mobile particles are localized on well-defined sites with equal energies. Diffusion occurs *via* thermally activated hopping processes over potential barriers. The basic assumption of the model is that the disorder causes a broad distribution of barrier heights.

Even in the case of non-interacting particles, the ac conductivity of random barrier model systems cannot be calculated analytically, but one has to resort to approximations[14–29]

or to numerical methods, *e.g.* to Monte Carlo computer simulations.[30,31] Recently, Schroder and Dyre developed a numerical method for calculating exact ac conductivity spectra at low temperatures where the maximum barrier height is much larger than the average thermal energy of the mobile particles.[32] They found that the shape of the model spectra is very similar to the experimental spectra of ion conducting glasses. The present author developed a Monte Carlo method for simulations of the particle dynamics at low temperatures.[33] One decisive result of these simulations was that the mean square displacement of the particle does not obey the scaling relation (2).

In this paper, we analyse these numerical results in more detail, in particular in comparison to the experimental results (A), (B) and (C). Additionally, we have performed simulations on the dynamics of particles which interact *via* long-range Coulomb forces. For these simulations, we have used the simulation method described in ref. 33. We find that the ac conductivity spectra of the interacting particles exhibit a number of features that we also observe in the conductivity spectra of ion conducting glasses.

We would like to note that the influence of Coulomb interactions on the particle dynamics in disordered potential landscapes was studied extensively by Maass, Bunde, Dieterich and coworkers.[34–36] However, their studies were restricted to relatively high temperatures, as they used standard Monte Carlo simulations. In their temperature range, they found that the presence of both disorder and Couloumb interactions is important for obtaining a strong dispersion of the ac conductivity. Here, we discuss the influence of Coulomb interactions at considerably lower temperatures, *i.e.* in the typical temperature range of ac impedance experiments. In this temperature range, the disorder is sufficient to produce a strong dispersion of the ac conductivity, while the influence of the Coulomb interactions on the conductivity spectra is quite sophisticated.

2. Monte Carlo method

The simulations were performed on three-dimensional cubic lattices of spacing a with periodic boundary conditions. The number of sites on the lattices was chosen between 17^3 and 23^3. Static random barrier potential landscapes were constructed as follows. The potential minima where the particles are located (particle sites) are all at the same energy level, while the energy barriers between these sites, $E_{A,i}$, are spatially uncorrelated random variables. Here, we have taken these variables from a boxcar distribution $P(E_{A,i}) = 1/E_{A,\max}$ with width $E_{A,\max}$.

We have assumed that a site can only be occupied by a single particle (hard-core repulsion). Additionally, repulsive Coulomb interactions between the particles were taken into account. These interactions are characterized by the parameter $V = q^2/(4\pi\varepsilon_0\varepsilon_{\text{eff}}a)$. Here, ε_0 and ε_{eff} are the permittivity of free space and an effective relative permittivity, respectively. In order to ensure overall charge neutrality, a uniform background is added. The effects of Coulomb interactions on the particle dynamics were now studied by varying the ratio $V/E_{A,\max}$ and the fraction of sites occupied by particles, c. In the following, the quantity c will be called the 'concentration' of the particles.

Furthermore, we have assumed that only nearest-neighbour hopping is possible. We have used the standard Metropolis algorithm[37] and have chosen the jump probabilities w_i as follows:

$$w_i = \exp(-E_{A,i}/kT)\min\{1, \exp(-\Delta E_c/kT)\}. \quad (3)$$

Here, ΔE_c is the difference between the Coulomb energy of a jumping particle at the target site and at the original site. In calculating ΔE_c, one has to take care of the image particles caused by the periodic boundary conditions, which is done by using Ewald's method.[38] After each elementary step of the simulation, the time t was incremented by τ_0/N, where N and τ_0 are the number of particles and a characteristic 'rattling time' in the potential minima, respectively.

After thermalization, the mean square displacement of the mobile particles

$$\langle r^2(t)\rangle = \frac{1}{N}\left\langle \sum_{i=1}^{N} \Delta \boldsymbol{r}_i^2(t) \right\rangle \quad (4)$$

and also the corresponding many-particle displacement function

$$\langle R^2(t)\rangle = \frac{1}{N}\left\langle \left(\sum_{i=1}^{N} \Delta \boldsymbol{r}_i(t) \right)^2 \right\rangle \quad (5)$$

were determined. From the mean square displacement $\langle r^2(t)\rangle$, a frequency-dependent coefficient of self-diffusion $\hat{D}(\nu)$ and a frequency-dependent single-particle conductivity $\hat{\sigma}_{1p}(\nu)$ were derived as follows:

$$\hat{D}(\nu) = \frac{i2\pi\nu}{6}\int_0^\infty \frac{\mathrm{d}\langle r^2(t)\rangle}{\mathrm{d}t}\exp(-i2\pi\nu t)\mathrm{d}t, \quad (6)$$

$$\hat{\sigma}_{1p}(\nu) = \frac{cq^2}{a^3kT}\hat{D}(\nu). \quad (7)$$

Accordingly, the conductivity diffusion coefficient $\hat{D}_\sigma(\nu)$ and the electrical conductivity $\hat{\sigma}(\nu)$ were derived from the function $\langle R^2(t)\rangle$:

$$\hat{D}_\sigma(\nu) = \frac{i2\pi\nu}{6}\int_0^\infty \frac{\mathrm{d}\langle R^2(t)\rangle}{\mathrm{d}t}\exp(-i2\pi\nu t)\mathrm{d}t, \quad (8)$$

$$\hat{\sigma}(\nu) = \frac{cq^2}{a^3kT}\hat{D}_\sigma(\nu). \quad (9)$$

In order to be able to obtain these functions also at low temperatures and on long timescales, we have used the 'modified landscape method' described in ref. 33. On short timescales, we have performed standard Monte Carlo simulations. For simulations on long timescales, we have modified the potential landscape in the following way. We have raised all barriers $E_{A,i}$ which are smaller than an arbitrarily chosen barrier height E_A^* to E_A^*. In this modified landscape, the hopping probability was chosen as $w_i = \exp(-(E_{A,i} - E_A^*)/kT)\ \min[1,\exp(-\Delta E_c/kT)]$ and after each elementary step of the simulation, the time t was incremented by τ^*/N with $\tau^* = \tau_0\exp(E_A^*/kT)$. Owing to this choice of the hopping probability and of the time steps, the simulation could be extended to longer timescales as compared to the original landscape. The decisive point is now that on timescales $t \gg \tau^*$, the functions $\langle r^2(t)\rangle$ and $\langle R^2(t)\rangle$ become indistinguishable in both landscapes.[33] Therefore, on timescales $t \gg \tau^*$, these functions could be taken from the modified landscape. Accordingly, by choosing different modified landscapes with different values of E_A^*, the simulations could be extended to more than 10^{20} Monte Carlo steps (particle)$^{-1}$. As explained in ref. 33, it is however important that E_A^* is considerably lower than the percolation barrier in a three-dimensional cubic lattice. Note that the application of percolation theory to the random barrier model will be discussed in Section 4.

For the calculation of $\hat{D}(\nu)$ and $\hat{\sigma}(\nu)$, the simulation results for $\langle r^2(t)\rangle$ and $\langle R^2(t)\rangle$, respectively, were fitted using 10th-order polynomials, and the polynomials were then Fourier-transformed according to eqns. (6)–(9).

3. Results

3.1. Model systems without Coulomb interactions between the particles

In ref. 33, results for the time-dependent mean square displacement of the mobile particles in a random barrier model (RBM) system without Coulomb interactions between the particles were presented. The concentration of the particles was chosen as $c = 0.01$, so that the effects of hard-core repulsion on the particle dynamics could be neglected. Since the movements of the particles are virtually independent, the functions $\langle r^2(t)\rangle$ and $\langle R^2(t)\rangle$ on the one hand and the functions $\hat{\sigma}_{1p}(\nu)$ and $\hat{\sigma}(\nu)$ on the other hand are virtually identical. We performed the simulations in a temperature range where the ratio $E_{A,\max}/kT$ varies between 60 and 140.

An analysis of the scaling properties of $\langle r^2(t)\rangle$ revealed that $\langle r^2(t)\rangle$ does not obey the scaling law (2). Consequently, the frequency-dependent conductivity $\hat{\sigma}(\nu)$ should not obey the scaling relation (1). As shown in Fig. 1, this is indeed the case. Here, we have scaled the frequency axis with $D_0 = D'(\nu \to 0)$ which is proportional to $\sigma_{dc}T$. Clearly, the isotherms of the real part of the conductivity, σ', are shifted to lower values on the ν/D_0 axis as the temperature decreases.

On the other hand, at frequencies below the high-frequency plateau, the shape of the σ' isotherms does not significantly depend on temperature. Therefore, the isotherms can be superimposed by introducing at additional scaling factor f for the frequency axis, see Fig. 2. The temperature dependence of the scaling factor f is approximately given by $f \propto T^{-1.3}$. Note that Schroder obtained very precise results for the temperature dependence of f in a single-particle RBM. He found that $f \propto T^{-(1.37 \pm 0.01)}$.[39]

In Fig. 3 we compare the low-frequency part of the conductivity master curve shown in Fig. 2 with the conductivity master curve of a 0.0051 $Na_2O \cdot 0.9949\ GeO_2$ glass. The master curve of the glass has been produced by plotting $\sigma'(\nu)/\sigma_{dc}$ *versus* $\nu/(\sigma_{dc}T)$. The random barrier master curve from Fig. 2 has been shifted onto the glass master curve by using an empirical scaling parameter g for the frequency axis. Although the theoretical and the experimental master curve were generated by using different scaling relations, the shapes of the master curve are very similar. This similarity was also found by Dyre and coworkers, see ref. 32.

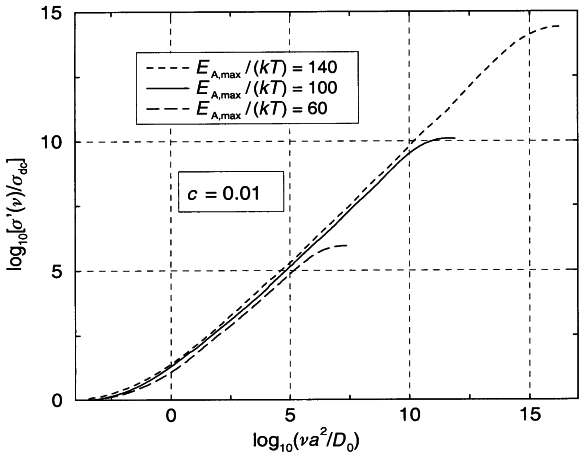

Fig. 1 Conductivity isotherms of a random barrier model system without Coulomb interactions between the particles. The isotherms are scaled according to eqn. (1).

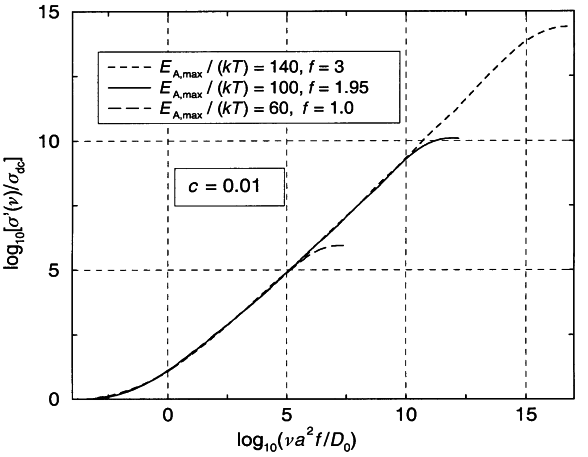

Fig. 2 Conductivity isotherms of a random barrier model system without Coulomb interactions between the particles. The isotherms are scaled by using an additional scaling factor $f \propto T^{-1.3}$.

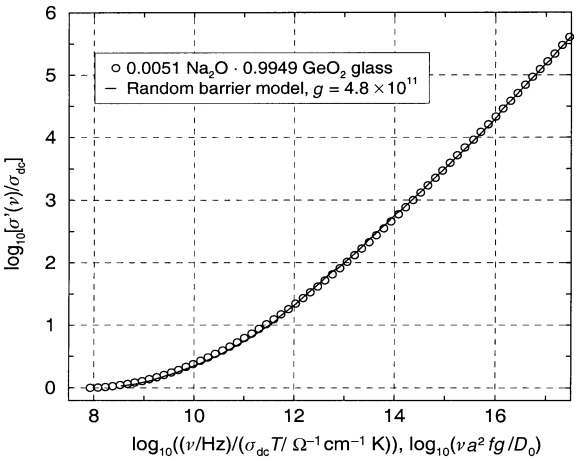

Fig. 3 Comparison between the conductivity master curves of a random barrier model system and of a sodium germanate glass. The random barrier master curve has been shifted onto the glass master curve by using an empirical scaling parameter $g = 4.8 \times 10^{11}$ for the frequency axis.

3.2. Model systems with Coulomb interactions between the mobile particles

When the mobile particles interact *via* long-range Coulomb forces, they do not move independently. In Fig. 4 we show $D(\nu)$ and $D_\sigma(\nu)$ curves obtained for the following simulation parameters: $c = 0.01$, $E_{A,\max}/kT = 60$, $V/kT = 100$. As seen from the figure, correlations between the motions of different particles become more pronounced as the frequency decreases. The Haven ratio $H_R = \lim_{\nu \to 0} D(\nu)/D_\sigma(\nu)$ is approximately 0.8. Note that for ion conducting glasses, the Haven ratio is found to vary between 1.0 at low number densities of mobile ions ($N_V < 10^{20}$ cm^{-3}) and roughly 0.2–0.4 at high number densities of mobile ions ($N_V \approx 10^{22}$ cm^{-3}).

Let us now consider the influence of the Coulomb interactions on the scaling properties of the real part of the conducitvity, $\sigma'(\nu)$. To do this, we choose a constant particle concentration $c = 0.01$ and a constant ratio $V/E_{A,\max} = 10/6$, and we change the temperature such that $E_{A,\max}/kT$ varies between 40 and 80. In Fig. 5 we scale the conductivity isotherms according to eqn. (1). Although the isotherms do not superimpose exactly, the shift between the isotherms is considerably smaller than for the random barrier model systems without Coulomb interactions, see Fig. 1.

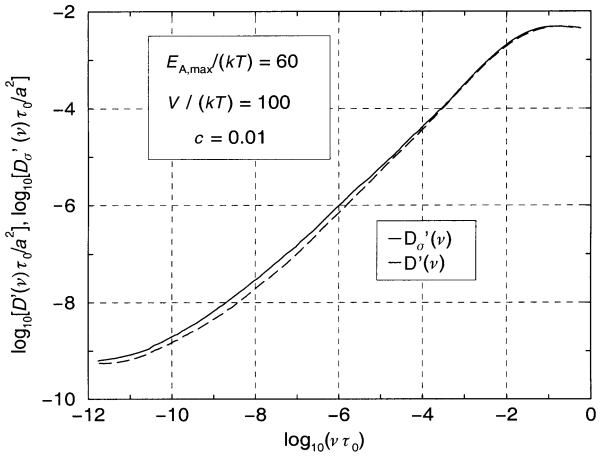

Fig. 4 Comparison between the diffusion coefficient $D'(\nu)$ and the conductivity diffusion coefficient $D_\sigma'(\nu)$ in a random barrier model system with Coulomb interactions between the mobile particles.

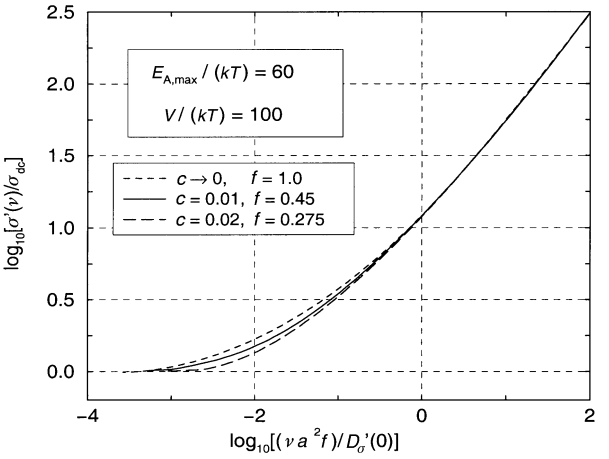

Fig. 6 Influence of the particle concentration on the shape of conductivity spectra in model systems with Coulomb interactions. The scaling factor f was chosen such that the spectra overlap at high frequencies.

Next, we examine in what way the particle concentration c influences the shape of the conductivity spectra. We choose $E_{A,max}/kT = 60$ and $V/kT = 100$ and vary the particle concentration between $c \to 0$ and $c = 0.02$. At very low particle concentrations $c \to 0$, Coulomb interactions do not play any role, and the shape of the conductivity spectrum is identical to that shown in Fig. 2. With increasing particle concentration, the shape changes slightly. In particular, the transition from the dc conductivity to the dispersive conductivity becomes more abrupt. Note that the same feature is observed when the alkali oxide content of ion conducting glasses is increased (experimental result (B)). In this context, it is remarkable that the so-called 'macroscopic model' by Dyre and Schroder[29,40,41] also yields a more abrupt transition from the dc to the dispersive conductivity than a RBM without Coulomb interactions. In this 'macroscopic model', Dyre and Schroder consider a heterogeneous solid with a spatially varying conductivity caused by free charge carriers. The interactions between the charge carriers are explicitly taken into account.

Finally, we analyse in what way the Coulomb interactions influence the characteristic mean square displacement where the subdiffusive behaviour of the mobile particles crosses over into diffusive behaviour, $\langle r_{cr}^2 \rangle$. Again, we choose $E_{A,max}/kT = 60$ and $V/kT = 100$, and we vary the particle concentration. In Fig. 7 we plot the typical length $\sqrt{\langle r_{cr}^2 \rangle}$ *versus* the particle concentration c. In a concentration range from 0.5% to 2%, $\sqrt{\langle r_{cr}^2 \rangle}$ decreases approximately with $c^{-1/3}$. This theoretical result is in agreement with the experimental result (C).

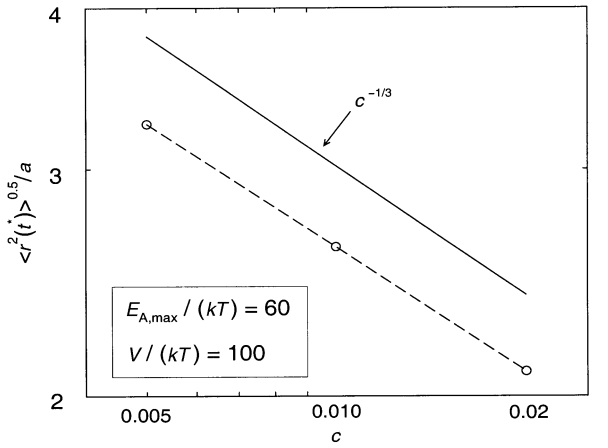

Fig. 7 Dependence of the typical length $\sqrt{\langle r_{cr}^2 \rangle}$ on the particle concentration c.

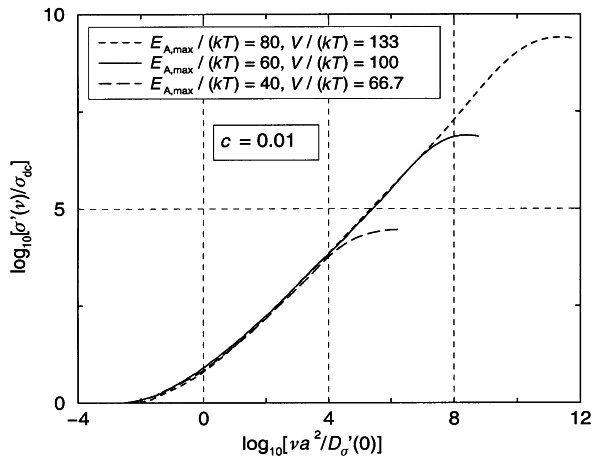

Fig. 5 Conductivity isotherms of a random barrier model system with Coulomb interactions between the particles. The isotherms are scaled according to eqn. (1).

4. Discussion

In the random barrier model systems without Coulomb interactions, we find that the frequency- and temperature-dependent conductivity obeys the following scaling relation:

$$\frac{\sigma'(\nu)}{\sigma_{dc}} = G\left(\frac{\nu}{\sigma_{dc}T}T^{-1.3}\right). \quad (10)$$

As seen from Fig. 3, the shape of the temperature-independent model function G is very similar to the experimental function F (eqn. (1)). The best analytical description of this shape seems to be the 'diffusion cluster approximation' formula given by Schroder and Dyre.[29,32] Note that the scaling relation (10) was predicted by Baranovskii and Cordes who calculated the conductivity of a single particle in the random barrier model by using a percolation approach.[42] In three-dimensional random barrier models, one can define a percolation barrier $E_{A,p}$ as follows:

$$\int_0^{E_{A,p}} P(E_A)\mathrm{d}E_A = p_c\,. \quad (11)$$

$p_c = 0.2488$ is the minimum fraction of barriers required to establish an infinite percolation cluster, *i.e.* to establish *one* continuous pathway for the mobile particle through the system.[43] In the case of a boxcar distribution of barrier heights, we have simply $E_{A,p} = 0.2488 E_{A,max}$. Now, Baranovskii and Cordes argue in the following way. If the mobile particle used exclusively barriers up to $E_{A,p}$ for diffusion, only *one* continuous pathway would exist. It would take a long time to find this pathway, since the infinite percolation cluster is fractal on all length scales. In order to have more diffusion pathways without including barriers considerably larger than $E_{A,p}$ into the pathways, the particles will use barriers up to approximately $E_{A,p} + kT$. This implies that the number of diffusion pathways and the correlation length of the percolation cluster, L_c, depends on temperature.[42] Using standard percolation theory, Baranovskii and Cordes find that the conductivity of the particle obeys the scaling relation

$$\frac{\sigma'(\nu)}{\sigma_{dc}} = H\left(\frac{\nu}{\sigma_{dc} T^{\lambda-\Delta}}\right). \qquad (12)$$

Here, $\lambda \approx 0.9$ and $\Delta \approx 2.2$ are critical exponents characterizing the topology of the infinite percolation cluster.[42] Although the shape of the scaling function H differs from that of the scaling function G we obtain in our simulations, the exponent $\lambda - \Delta$ is virtually identical to our exponent -1.3. In contrast, in the case of ion conducting glasses, this exponent is found to be close to zero (experimental result (A)).

Furthermore, it is obvious that the random barrier model without Coulomb interactions is not able to account for the experimental results (B) and (C). At low particle concentrations, the hard-core repulsion between the particles does neither lead to a significant concentration dependence of the spectral shape of the conductivity nor to a significant concentration dependence of $\langle r_{cr}^2 \rangle$.

Let us now consider in comparison the situation in random barrier model systems with Coulomb interactions between the mobile particles. In Fig. 5, we have shown scaled conductivity isotherms for a system with $c = 0.01$ and $V/E_{A,max} = 10/6$. In this system, the average interaction strength between the particles is $\bar{V} \approx Va/d$ with $d/a = 2 \times (3/4\pi c)^{1/3}$. d denotes an estimate for the average distance between the particles in units of the lattice spacing a. Inserting $c = 0.01$, we obtain $\bar{V} \approx 0.17$ $V \approx 0.29 E_{A,max} \approx 1.16 E_{A,p}$. That means the average interaction strength is comparable to the height of the percolation barrier. In this case, we observe that the scaling properties of the conductivity are close to the scaling properties of the experimental spectra as described by eqn. (1).

When we increase the interaction strength in the model systems by increasing the particle concentration, we observe slight changes in the shape of the conductivity spectra (Fig. 6) and a decrease in the characteristic length $\sqrt{\langle r_{cr}^2 \rangle}$ (Fig. 7), in close agreement with the experimental results (B) and (C). Thus, we can state that the particle dynamics in the random barrier model systems with Coulomb interactions exhibit a number of features we also observe for the ion dynamics in glasses.

In the following, we would like to propose a simple qualitative picture describing the possible influence of the Coulomb interactions on the particle dynamics. On short timescales, the effective potential a mobile particle 'feels' is a superposition of the static random barrier potential and a Coulomb potential due to the repulsion of the other mobile particles. When the Coulomb repulsion is strong, the particles tend to distribute homogenously over the system. In his 'concept of mismatch and relaxation' (CMR), Funke approximates the Coulomb potential 'felt' by a mobile particle by an harmonic cage potential.[44,45] Here, we adopt this idea, and in Fig. 8, we sketch the resulting effective potential in random barrier model systems. In the energetically favored situation, the mobile particle we consider is located close to the minimum of the effective potential. However, the position of this minimum shifts when other particles change their positions.

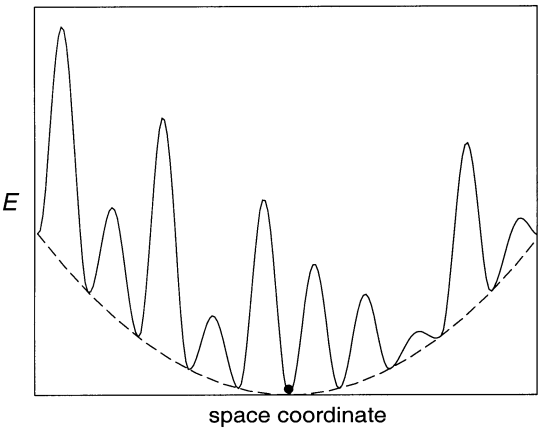

Fig. 8 Effective single-particle potential in a random barrier model system with Coulomb interactions between the mobile particles. The dashed line denotes a cage potential due to the Coulomb repulsion of neighbouring particles. Of course, this single-particle potential applies only on short time scales.

How will the particle dynamics in this effective potential differ from the particle dynamics in a random barrier model without Coulomb interactions? On short timescales when the root mean square displacement of the particles is smaller than the lattice spacing a, the minimum of the effective potential should still be close to the original site of the particle. This implies that with increasing distance from this site, the site energies increase and the occupation numbers of the sites decrease. When the particle now begins to explore (*i.e.* to visit) its neighboring sites, it will stay only for short time intervals on high-energy sites. The short stays on these sites will, therefore, not contribute much to the mean square displacement of the particle. Consequently, on a timescale where the particle is able to explore a spatial area of the order of the correlation volume of the percolation cluster, $(L_c)^3$, the mean square displacement of the particle will be considerably smaller than $(L_c)^2$ due the small occupation numbers of the higher-energy sites. On the other hand, it is clear that as soon as the particles are able to explore a spatial area of the order of $(L_c)^3$, the subdiffusive behaviour of the particles passes over into diffusive behaviour, since the particles no longer move within isolated clusters, but begin to perform diffusive long-range motions. This leads to a rapid growth of the mean square displacement.

Thus, the Coulomb interactions should lead to a decrease in the mean square displacement on timescales where the spatial area the particle explore is smaller than $(L_c)^3$. Accordingly, with increasing strength of the interactions, the value of $\langle r_{cr}^2 \rangle$ should decrease (Fig. 7) and the transition from subdiffusive behaviour into diffusive behaviour should become more abrupt (Fig. 6).

Of course, the Coulomb interactions should also affect the scaling properties of the conductivity isotherms for a given particle concentration (compare Fig. 1 and 5). In a random barrier model without Coulomb interactions, $\langle r_{cr}^2 \rangle$ is determined by the temperature-dependent topology of the infinite percolation cluster. This leads to the scaling law (12). In contrast, in a model with Coulomb interactions, the value of $\langle r_{cr}^2 \rangle$ is strongly influenced by the strength of the interactions, see the above considerations. Thus, the temperature-dependent topology of the infinite percolation cluster plays a less important role. Obviously, this leads to a reduction in the temperature dependence of $\langle r_{cr}^2 \rangle$ in comparison to a random barrier model without Coulomb interactions.

Finally, we would like to emphasize that this simple picture should be considered a first approach to obtaining a better

understanding of the influence of Coulomb interactions on the particle dynamics. Here, more theoretical work is clearly needed.

5. Summary

We have performed Monte Carlo simulations of the particle dynamics in random barrier model systems with and without Coulomb interactions between the mobile particle. The temperature range of these simulations covers the typical temperature range of ac impedance experiments. We have analysed the conductivity spectra of the model systems in comparison to the spectra of ion conducting glasses. A decisive result is that the interactions give rise to a number of features in the model spectra which we also observe in the spectra of ion conducting glasses. We discuss the influence of the Coulomb interactions on the particle dynamics in the random barrier model, and we suggest that the interactions considerably reduce the mean square displacements of the mobile particles on timescales where the spatial area the particle explore is smaller than the correlation volume of the percolation cluster.

Acknowledgements

The author would like to thank R. Banhatti and A. Heuer for critically reading the manuscript and for helpful discussions. Financial support by the Deutsche Forschungsgemeinschaft *via* the Sonderforschungsbereich 458 is also gratefully acknowledged.

References

1 J. E. Kelly III, J. F. Cordaro and M. Tomozawa, *J. Non-Cryst. Solids*, 1980, **41**, 47.
2 G. E. Murch, *Solid State Ionics*, 1982, **7**, 177.
3 K. Funke, *Prog. Solid State Chem.*, 1993, **22**, 111.
4 E. Bychkov, V. Tsegelnik, Yu. Vlasov, A. Pradel and M. Ribes, *J. Non-Cryst. Solids*, 1996, **208**, 1.
5 J. O. Isard, *J. Non-Cryst. Solids*, 1999, **246**, 16.
6 B. Roling, C. Martiny and K. Funke, *J. Non-Cryst. Solids*, 1999, **249**, 201.
7 J. C. Kimball and L. W. Adams, Jr., *Phys. Rev. B*, 1978, **18**, 5851.
8 B. Roling, *Solid State Ionics*, 1998, **105**, 185.
9 B. Roling and C. Martiny, *Phys. Rev. Lett.*, 2000, **85**, 1274.
10 J. N. Mundy, G. L. Jin and N. L. Peterson, *J. Non-Cryst. Solids*, 1986, **84**, 320.
11 H. Kahnt, *J. Non-Cryst. Solids*, 1996, **203**, 225.
12 D. L. Sidebottom, P. F. Green and R. K. Brow, *J. Non-Cryst. Solids*, 1997, **222**, 354.
13 D. L. Sidebottom, *Phys. Rev. Lett.*, 1999, **82**, 3653.
14 M. Pollak and T. H. Geballe, *Phys. Rev.*, 1961, **122**, 1742.
15 B. I. Shklovskii and A. L. Efros, *Sov. Phys. JETP*, 1971, **33**, 468.
16 V. Ambegaokar, B. I. Halperin and J. S. Langer, *Phys. Rev. B*, 1971, **4**, 2612.
17 E. W. Montroll and H. Scher, *J. Stat. Phys.*, 1973, **9**, 101.
18 H. Scher and E. W. Montroll, *Phys. Rev. B.*, 1975, **12**, 2455.
19 S. Alexander and R. Orbach, *Physica B*, 1981, **107b**, 675.
20 S. Summerfield, *Solid State Commun.*, 1981, **39**, 401.
21 T. Odagaki and M. Lax, *Phys. Rev. B*, 1981, **24**, 5284.
22 I. Webman, *Phys. Rev. Lett.*, 1981, **47**, 1496.
23 S. Tye and B. I. Halperin, *Phys. Rev. B*, 1989, **39**, 877.
24 P. L. Doussal, *Phys. Rev. B*, 1989, **39**, 881.
25 J. C. Dyre, *J. Appl. Phys.*, 1988, **64**, 2456.
26 J. C. Dyre, *Phys. Rev. B*, 1994, **49**, 11 709.
27 J. C. Dyre, *Chem. Phys.*, 1996, **212**, 61.
28 J. C. Dyre and T. B. Schroder, *Phys. Rev. B*, 1996, **54**, 14 884.
29 J. C. Dyre and T. B. Schroder, *Rev. Mod. Phys.*, 2000, **72**, 873.
30 P. Argyrakis, A. Milchev, V. Pereyra and K. W. Kehr, *Phys. Rev. E*, 1995, **52**, 3623.
31 A. Hörner, A. Milchev and P. Argyrakis, *Phys. Rev. E*, 1995, **52**, 3570.
32 T. B. Schroder and J. C. Dyre, *Phys. Rev. Lett.*, 2000, **84**, 310.
33 B. Roling, *Phys. Rev. B*, 2000, **61**, 5993.
34 P. Maass, J. Petersen, A. Bunde, W. Dieterich and H. E. Roman, *Phys. Rev. Lett.*, 1991, **66**, 52.
35 P. Maass, M. Meyer and A. Bunde, *Phys. Rev. B*, 1995, **51**, 8164.
36 P. Maass, M. Meyer, A. Bunde and W. Dieterich, *Phys. Rev. Lett.*, 1996, **77**, 1528.
37 N. Metropolis, A. W. Rosenbluth, M. N. Rosenbluth, A. H. Teller and E. Teller, *J. Chem. Phys.*, 1953, **21**, 1087.
38 M. P. Allen and D. J. Tildesley, *Computer Simulation of Liquids*, Clarendon Press, Oxford, 1987 .
39 T. B. Schroder, Dissertation, IMFUFA, Roskilde University, 1999.
40 J. C. Dyre, *Phys. Rev. B*, 1993, **48**, 12 511.
41 J. C. Dyre, *Phys. Rev. B*, 1993, **47**, 9128.
42 S. D. Baranovskii and H. Cordes, *J. Chem. Phys.*, 1999, **111**, 7546.
43 D. Stauffer and A. Aharony, *Introduction to Percolation Theory*, Taylor & Francis, London, 2nd rev., 1994, p. 17.
44 K. Funke and D. Wilmer, *Mater. Res. Soc. Symp. Proc.*, 1999, **548**, 403.
45 K. Funke and D. Wilmer, *Solid State Ionics*, 2000, **136**, 1329.